

Pesticide-Loaded Nanocarriers from Lignin Sulfonates—A Promising Tool for Sustainable Plant Protection

Sebastian Beckers, Stefan Peil, and Frederik R. Wurm*

Cite This: *ACS Sustainable Chem. Eng.* 2020, 8, 18468–18475

Read Online

ACCESS |



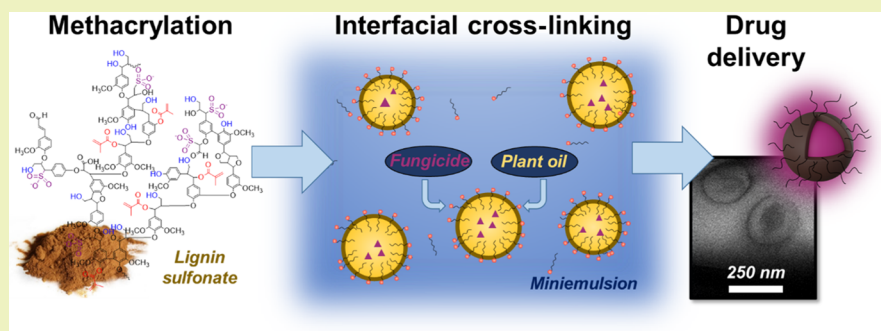
Metrics & More



Article Recommendations



Supporting Information



ABSTRACT: Lignin is a promising feedstock in sustainable formulations for agrochemicals not only because of its biodegradability but also because the biopolymer occurs naturally in the cell wall of plants and therefore is renewable and abundant. We used different lignin sulfonates to prepare stable aqueous dispersions of lignin nanocarriers loaded with agrochemicals by interfacial cross-linking in a direct miniemulsion. Despite the differences in structure and functionality, different lignin sulfonates were successfully methacrylated and degrees of methacrylation (>70%) were achieved. The resulting methacrylated lignin sulfonates were water-soluble and exhibited interfacial activity; they were used as reactive surfactants to stabilize oil droplets (cyclohexane or olive or rapeseed oil) loaded with a dithiol cross-linker [EDBET, 2,2'-(ethylenedioxy)bis(ethylthiol)] and a hydrophobic cargo (the fluorescent dye 1,3,5,7-tetramethyl-8-phenyl-4,4-difluoroboradiazaindacene or the commercial fungicides prothioconazole and pyraclostrobin). After the addition of a water-soluble base, the thia-Michael addition was initiated at the droplet interface and produced lignin sulfonate nanocarriers with a core-shell structure within oily core and a cross-linked shell. Nanocarriers with diameters of ca. 200–300 nm were prepared; encapsulation efficiencies between 65 and 90% were achieved depending on the cargo. When the amount of the cross-linker was varied, the resulting lignin nanocarriers allowed a controlled release of loaded cargo by diffusion over a period of several days. The strategy proves the potential of lignin sulfonates as a feedstock for delivery systems for advanced plant protection.

KEYWORDS: nanocarriers, lignin, emulsion polymerization, drug delivery, agriculture

INTRODUCTION

Over 4 million tons of pesticides are used annually to protect crops worldwide.¹ The conventional method to distribute pesticides in agriculture is spraying of agrochemical formulations. These formulations often encapsulate the active ingredients in petroleum-based, nondegradable polymer microcapsules to ensure sustained release of the actives.² These formulations are a major part of the intentionally added microplastics that reach the environment today. With current concerns about food insecurities and ineffective agricultural delivery of agrochemicals, the development of biodegradable and effective drug delivery vehicles for agriculture becomes an important area of research.^{3,4}

Lignin is the second most abundant biopolymer on earth, which can be extracted from the cell wall of terrestrial plants.⁵ Although lignin is available on a million ton scale, only 2% of the worldwide lignin production is processed to value-added

products, while the majority is incinerated.^{6,7} As lignin is stable against hydrolysis but can be degraded by certain fungi, it is an interesting material to prepare delivery systems for agriculture.^{8,9} Several studies used lignin and lignin sulfonates for the sustained release of fertilizers, pesticides, or drugs.^{10–13} However, to date, chemically modified lignin sulfonates have not been used in a direct emulsion to prepare cross-linked and agrochemical-loaded nanoparticles, which is reported in this manuscript.

Received: August 12, 2020

Revised: November 10, 2020

Published: December 8, 2020



Lignin is composed of three phenolic building blocks 4-hydroxyphenyl-, guaiacyl-, and syringyl alcohol, which are cross-linked in different ratios by a variety of ether-based binding motifs.^{6,14} Lignin is extracted from lignocellulosic biomass by different procedures and different soluble forms are currently available: Kraft lignin (KL), organosolv lignin (OL), or lignin sulfonates are the most common derivatives.^{6,14} However, the structural complexity of the hyperbranched polyether polyols, which depends on plant source and extraction method, have hindered the utilization in industrial production processes until now.^{5,15} Nevertheless, recently lignin received increased attention as a sustainable carrier material for agricultural formulations because of its biocompatibility, biodegradability, and UV absorbance.¹⁶

Most lignin carrier systems are based on the entrapment of an active ingredient during a lignin precipitation, which is induced either by addition of a precipitation agent or by solvent evaporation.^{16,17} A strategy that is more advanced and that allows tailoring of the product properties is the encapsulation of pesticides by cross-linking in a miniemulsion.¹⁸ Here, nanodroplets are dispersed in a continuous phase and form nanoscopic, individual batch reactors that allow a broad range of reactions to prepare nanomaterials with high encapsulation efficiency (EE).¹⁹ Recently, our group cross-linked unmodified lignin sulfonate at the droplets' interface of a water-in-oil miniemulsion with toluene diisocyanate to yield lignin-polyurethane nanocarriers with a core-shell structure, representing the first chemically cross-linked and degradable lignin nanocarriers.^{20,21} However, a redispersion step to transfer the dispersion into water was essential; also, isocyanates are highly reactive and might undergo unwanted side reactions with various cargo molecules. Alternative strategies attached reactive functional groups to lignin, which also enabled a covalent cross-linking: Chen et al. etherified lignin sulfonate with allyl bromide and converted it at the interface by a radically induced thiol-ene reaction in an oil-in-water (O/W) miniemulsion.²² However, high amounts of a radical initiator were needed to overcome lignin's radical scavenger properties, which limits this type of chemistry. In addition, the resulting nanocarriers quickly released the majority of the encapsulated cargo, indicating a relatively low cross-linking density. In contrast, nanocarriers that only released their cargo upon an enzymatic trigger were prepared from methacrylated KL,^{8,23} which was efficiently cross-linked via nucleophilic, instead of radical, chemistry. As KL is mainly incinerated directly after the pulping process, it is available on a smaller scale for additional chemical modification.^{14,24} In contrast, lignin sulfonates are available on a large scale (production volume: 7 million tons yearly) at low cost.²⁵ Thus, an efficient cross-linking chemistry to prepare lignin-sulfonate-based nanocarriers is desirable. As lignin sulfonates are produced by the sulfite process, during which sulfonation occurs, amphiphilic polymers are obtained.^{15,26} They are approved as emulsifiers for agricultural applications in Europe and thus an ideal feedstock for developing nanocarriers for plant protection.¹⁵

We utilized the amphiphilicity of lignin sulfonates to tailor a cross-linking process at a droplets' interface by a nucleophilic Michael addition. We describe the preparation of cross-linked lignin sulfonate nanocarriers loaded with oils (cyclohexane, toluene, or plant oils) and a commercial fungicide (pyraclostrobin or prothioconazole) and study their release profiles. Several lignin sulfonates were methacrylated and analyzed in

detail. The resulting water-soluble methacrylated lignin sulfonates were dissolved in the continuous phase of an O/W miniemulsion and cross-linked at the droplet interface because of their amphiphilicity. Stable aqueous dispersions containing lignin nanocarriers with a core-shell structure that were *in situ* loaded with fungicides were obtained, which released the actives over an adjustable time depending on the degree of cross-linking. Besides previously proven enzymatic degradability of lignin nanocarriers, this formulation might be used as a controlled release system of agrochemicals for sustainable crop protection by time-controlled diffusion for trunk injection or spraying applications.

■ EXPERIMENTAL SECTION

Materials. Lithium chloride (99%), triethylamine (TEA) (99%), 1,3,5,7-tetramethyl-8-phenyl-4,4-difluoroboradiazaindacene (Bodipy 326/515), methacrylic anhydride (95%), sodium dodecylsulfate (SDS, 99%), 2-chloro-4,4,5,5-tetramethyl-1,3,2-dioxaphospholane (95%), prothioconazole (analytical standard), *endo-N*-hydroxy-5-norbornene-2,3-dicarboximide (98%), chrome(III)acetylacetonate (97%), 2,2'-(ethylenedioxy)bis(ethylthiol) (EDBET, 95%), KL (alkaline product number: 370959), LSCa (lignin sulfonic acid calcium salt, product number: 47054), LSCH (sugared lignin sulfonic acid sodium salt, product number: 47011), and LSNa2 (lignin sulfonic acid sodium salt, product number: 471038) were obtained from Sigma-Aldrich. LSNa1 (lignin sulfonic acid sodium salt, product number: 8999-1) was bought from Carl Roth and LSNa3 (lignin sulfonic acid sodium salt, product number: L0098) was a product of TCI Chemicals. OL (product number: CP8068-03-9) was obtained from Chemical Point. Pyraclostrobin was purchased from Toronto Research Chemicals. Rapeseed oil produced from Rapso was used.

Methods. *Nuclear Magnetic Resonance Spectroscopy.* ¹H-, ¹H-¹³C-HSQC-, and ³¹P nuclear magnetic resonance (NMR) spectroscopy was performed using a Bruker AVANCE (USA) spectrometer at 300 MHz. In the case of ¹H measurements, the NMR sample contained 10 mg of dried lignin dissolved in 600 μ L of D₂O. For ¹H-¹³C-HSQC-spectra, ca. 40 mg of the sample was dissolved in 600 μ L of DMSO-*d*₆. Lignin's hydroxyl groups were quantified by ³¹P NMR after derivatization with 2-chloro-4,4,5,5-tetramethyl-1,3,2-dioxaphospholane in a CDCl₃-pyridine-*d*₅ (4/6 v/v ratio) mixture in the presence of the internal standard *endo-N*-hydroxy-5-norbornene-2,3-dicarboximide and the relaxation agent Cr(III)acetylacetonate using the method of Balakshin and Capanema.²⁷ Error values were determined from three different samples.

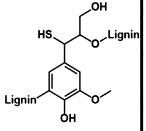
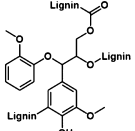
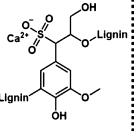
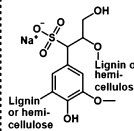
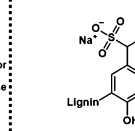
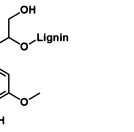

Fourier Transform Infrared Spectroscopy. Fourier transform infrared (FTIR) spectroscopy was performed using a Nicolet iS10 spectrometer with a Vertical ATR Accessory. The spectra were recorded between 600 and 4000 cm⁻¹. For the analysis of nanocarriers, a dispersion (2 mL) was centrifuged and the pellet was washed twice with water (10 mL) to remove the non-cross-linked lignin and SDS. Afterward, the dispersion was washed with cyclohexane (10 mL) in order to remove excess EDBET by vigorous shaking of the mixture and subsequent centrifugation to fasten the phase separation. Finally, the purified dispersion was freeze-dried.

Size Exclusion Chromatography. The molecular weight of the lignin sulfonates was determined using a mixture of sodium hydroxide solution (0.1 M) and 20% acetonitrile as an eluent. The measurement was performed at an Agilent 1100 Series (Agilent Technologies 1260 Infinity) system using two PSS MCX columns (1k, 100k) and a UV detector (270 nm) at a flow rate of 1 mL/min.

Inductively Coupled Plasma Emission Spectroscopy. The sulfur content of aqueous 0.1 N NaOH solutions containing 1 mg/mL of lignin was determined by spectral lines at 180 nm and 182 nm using an Activa M spectrometer from Horiba. Error values were calculated from two samples each three replicates.

Dynamic Light Scattering. Dynamic light scattering (DLS) was performed on a Zetasizer Nano S90 submicron particle sizer (Malvern

Table 1. Structural Properties of Several Lignin Sulfonates in Comparison to KL and OL^a

Structure	Kraft lignin	Organsolv lignin	Lignin sulfonates (LS)				
							
Code	KL	OL	LSCa	LSCH	LSNa1	LSNa2	LSNa3
Supplier	Sigma Aldrich (370959)	Chemical Point (CP8068-03-9)	Sigma Aldrich (47054)	Sigma Aldrich (47011)	Carl Roth (8999-1)	Sigma Aldrich (471038)	TCI (L0098)
c(OH) total mmol/g	6.6±0.2	4.5±0.1	12.6±0.1	20.2±0.2	13.2±0.1	8.1±0.3	19.9±0.2
c(OH) arom mmol/g	4.3±0.2	2.8±0.1	4.9±0.1	3.6±0.1	1.7±0.1	2.3±0.1	4.5±0.2
c(OH) aliph mmol/g	2.4±0.2	1.6±0.1	7.8±0.1	16.7±0.2	11.5±0.1	5.9±0.2	15.4±0.2
c(COOH) mmol/g	0.5±0.1	2.0±0.1	n.d.	n.d.	n.d.	n.d.	n.d.
Sulfur mmol/g	0.5±0.01	0±0.01	2.7±0.01	1.6±0.01	1.6±0.01	2.0±0.01	1.9±0.02
Solubility	DMF, pyridine, DMSO, alkali	different org. solvents	water (pH 0-14)	water (pH 0-14), DMF, DMSO		water (pH 0-14)	

^aThe hydroxyl and carboxyl groups were determined with ³¹P NMR after phosphorylation.²⁷ ICP-OES was performed to quantify the sulfur content.

Panalytical, UK) at a fixed angle of 90° and a laser diode running at 633 nm.

Transmission Electron Microscopy. The transmission electron microscopy (TEM) specimen was stained with uranyl acetate, and a drop of sample solution was placed onto a carbon-coated copper grid. A Tecnai F20 device from FEI was used at an acceleration voltage of 200 kV.

Tensiometry (Spinning Drop Method). The interfacial tension between cyclohexane and water was measured with a spinning drop tensiometer (SVT 20N from DataPhysics). A glass capillary was filled with cyclohexane and a small droplet of Milli-Q water (as a reference) or an aqueous solution containing 5 mg/mL of methacrylated lignin sulfonate. Then, the capillary was placed horizontally and equilibrated at 20 °C for 10 min under rotation at 8000 rpm until a cylindrical droplet at the axis of rotation was obtained. The interfacial tension based on the theory of Cayias, Schechter, and Wade was used for data analysis.

High-Pressure Liquid Chromatography. Before measurement, all samples were passed through a 0.2 μm filter and analyzed by an Agilent Eclipse Plus RP18 HPLC system using tetrahydrofuran/water/0.1 %wt as the mobile phase and a trifluoroacetyl gradient. The injection volume was 10 μL and the column temperature was maintained at 20 °C. The analysis was performed at a flow rate of 0.2 mL/min with the UV detector at 280 nm for pyraclostrobin and 260 nm for prothioconazole.

Fluorescence Spectroscopy. Bodipy 326/515 was quantified by its fluorescence (ex.: 326 nm; em.: 515 nm) using a TECAN infinite M1000 Microplate reader.

Determination of EE and Release of the Cargo. In order to determine the EE, two approaches were used: (A) 0.5 mL of a 10 mg/mL nanocarrier suspension was centrifuged at 14k rpm (Eppendorf centrifuge 5424; 18,407 rcf) for 30 min (at 20 °C) and a nonencapsulated amount of cargo was quantified from the supernatant. (B) Cyclohexane (0.25 mL) was added to 0.25 mL of a loaded nanocarrier suspension. The two-phase mixture was shaken for 30 s to transfer the free cargo, which could not be encapsulated, to the cyclohexane phase. To fasten the phase separation, the mixture was centrifuged (14k rpm, 18,407 rcf, 30 min) subsequently. To record the release kinetics, the EE was measured after 2, 4, and 7 days using

method B. Bodipy 326/515 transferred to the cyclohexane phase was quantified photometrically by its fluorescence, whereas prothioconazole and pyraclostrobin were quantified by high-pressure liquid chromatography (HPLC). The EE (EE %) was calculated using eq 1; assuming an inaccuracy of 5% during pipetting, the typical error values for EE are found to be ca. 0.5% using this strategy.

$$EE \% = \frac{c(\text{cargo initial}) - c(\text{cargo in supernatant})}{c(\text{cargo initial})} \times 100\% \quad (1)$$

Syntheses. Methacrylation of Lignin Sulfonates. Lignin sulfonate (1 g, for a number of hydroxyl groups, see Table 1) was added to 15 mL of dimethyl formamide (DMF) and 1.35 g of LiCl. Subsequently, 0.45 mL of TEA and 1.7 equiv of methacrylic anhydride (relative to lignin's hydroxyl groups) were added dropwise, and the reaction was allowed to proceed at 65 °C overnight under stirring. The mixture was precipitated into 300 mL of diethyl ether and isolated by centrifugation (10k rpm, 30 min). The solid was washed twice with diethyl ether. The product was dried at 40 °C *in vacuo* characterized with FTIR, ¹H-, and ¹H-¹³C-HSQC spectroscopy as well as by size exclusion chromatography (SEC) subsequently. The hydroxyl group conversion (determined by ³¹P NMR²⁷) is summarized in Table 2. Yields: typically >95%.

Table 2. Conversion of Hydroxyl Groups of Different Lignin Batches Determined with ³¹P NMR after Phosphorylation According to a General Literature Protocol (MA = Methacrylate Group)^{27a}

no.	lignin	X % _{arom} OH	X % _{aliph} OH	X % _{total} OH	n(MA)/mmol g ⁻¹
1	LSCH	90 ± 1	89 ± 1	90 ± 1	18 ± 1
2	LSCa	95 ± 1	93 ± 1	95 ± 1	12 ± 1
3	LSNa1	100 ^a	95 ± 1	96 ± 1	13 ± 1
4	LSNa2	73 ± 1	72 ± 1	73 ± 1	6 ± 1
5	LSNa3	90 ± 1	87 ± 1	90 ± 1	18 ± 1

^aNo residual signal was detected.

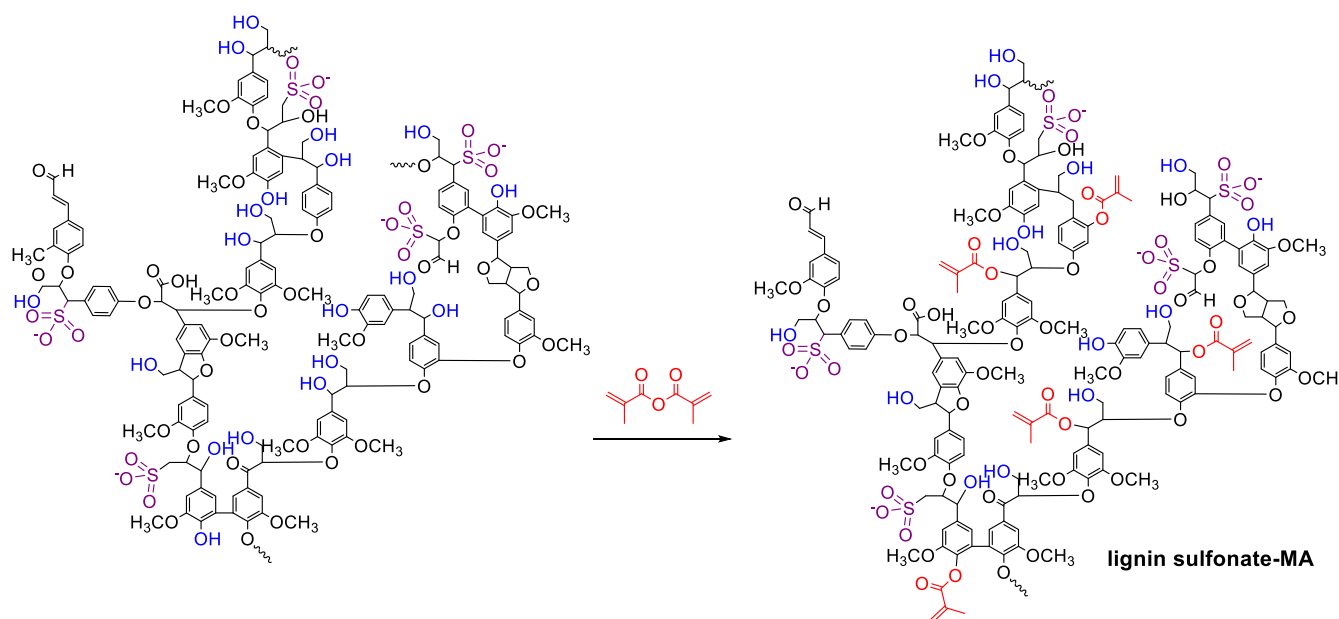


Figure 1. Functionalization of lignin sulfonates with methacrylic anhydride. The shown chemical structure represents typical lignin binding motifs.

Preparation of Lignin Nanocarriers from Methacrylated Lignin Sulfonate. Cross-linked lignin nanocarriers were prepared by interfacial cross-linking in an O/W miniemulsion. Typically, 50 mg of methacrylated lignin sulfonate (LSNa1-MA; 0.64 mmol methacrylated groups) and 44 μL (0.32 mmol) of TEA were dissolved in 5 mL of Milli-Q water. Afterward, a solution of 122 μL of cyclohexane or rapeseed oil, 56 μL (0.69 mmol SH groups) of EDBET, and a hydrophobic cargo such as prothioconazole (2.5 mg), pyraclostrobin (2.5 mg), or Bodipy 326/515 (0.0122 mg, using a stock solution) was added. Immediately, the two-phase mixture was sonicated for 3 min (Branson Sonifier W450 Digital, one half-inch tip 1/2 in. tip, 70% amplitude, 20 s ultrasound, followed by 10 s pause) under ice cooling to prevent premature cross-linking. Subsequently, the reaction was allowed to proceed for 24 h at 50 $^{\circ}\text{C}$ under stirring to yield a stable, brownish dispersion. For purification, the dispersion was centrifuged at 4000 rpm for 30 min. The obtained pellet was washed with water twice to remove non-cross-linked methacrylated lignin sulfonate and free drug. The dispersion was characterized by DLS and TEM.

RESULTS AND DISCUSSION

Characterization of Different Lignin Sulfonates. To find the optimal starting material, we characterized lignin sulfonic acid sodium salts from three different suppliers (LSNa1–3), one calcium lignin sulfonate (LSCa), and one “sugared” lignin sulfonic acid sodium salt (LSCH), containing hemicellulose residues, regarding their chemical structure and properties. For comparison, additional KL and OL were investigated (Table 1). The lignin sulfonates exhibited high water solubility in acidic as well as alkaline media but were insoluble in most organic solvents. The only exception was the sugared lignin sodium sulfonate LSCH, which was also soluble in polar solvents such as dimethyl sulfoxide (DMSO) and DMF. The high water solubility distinguishes lignin sulfonates from other lignin types such as KL or OL and is a result of the high number of polar hydroxyl and sulfonic acid groups.²⁸ The number of the latter was estimated by the sulfur content quantified by inductively coupled plasma emission spectroscopy (ICP-OES) and was typically between 1.6 and 2.0 mmol/g. ³¹P NMR was used after phosphorylation following the method of Balakshin and Capanema to determine the amount of hydroxyl groups (Figure S1A).²⁷ In comparison to KL and

OL, all the tested lignin sulfonates showed a relatively high amount of aliphatic hydroxyl groups (e.g., up to 16.66 mmol/g for LSCH) most likely because of higher content of hemicellulose residues. The significant difference between LSNa1, 2, and 3 regarding their total hydroxyl number but also in the varying ratio between phenolic and aliphatic OH groups underlines the structural diversity of the material even when isolated under comparable extraction conditions.

Methacrylation of Lignin Sulfonates. To prepare agrochemical-loaded lignin nanocarriers, we functionalized different lignin sulfonates with reactive methacrylate groups by esterification with methacrylic anhydride (Figure 1). Yiamsawas et al. reported the methacrylation of KL using excess of methacrylic anhydride (1.7 equiv with respect to lignin’s OH groups), TEA as a catalyst, and DMF as a reaction solvent.⁸ We investigated if these reaction conditions are transferable to the modification of lignin sulfonates. In contrast to the established protocol, most lignin sulfonates were functionalized in suspension because of their insolubility in typical organic solvents; however, good conversion was also achieved under these conditions (i.e., when 1.7 equiv of methacrylic anhydride was used). After the reaction, the modified lignin sulfonates were precipitated into diethyl ether with yields of typically above 95%.

After methacrylation, the water solubility of the lignin sulfonates decreased because of a reduction of hydroxyl groups and thus also of hydrogen bonds. By ¹H and ¹H–¹³C HSQC-NMR spectroscopy, the successful functionalization with methacrylates was proven (Figures S2 and S3). The ¹H NMR spectra (solvent: D₂O) showed two resonances between 5.2 and 5.7 ppm corresponding to the protons of the C=C double bond of the methacrylates. They were also detected at 125–128 ppm (¹³C) and in the respective ¹H–¹³C HSQC 2D-spectra (solvent: DMSO). Additionally, after methacrylation, we observed the shift, for example, of the signal belonging to the (CH₂) γ of the β -O-4-lignin binding motif in comparison to unmodified lignin sulfonate, indicating a successful methacrylation. The degree of functionalization was determined by ³¹P NMR after phosphorylation of the reaction product according

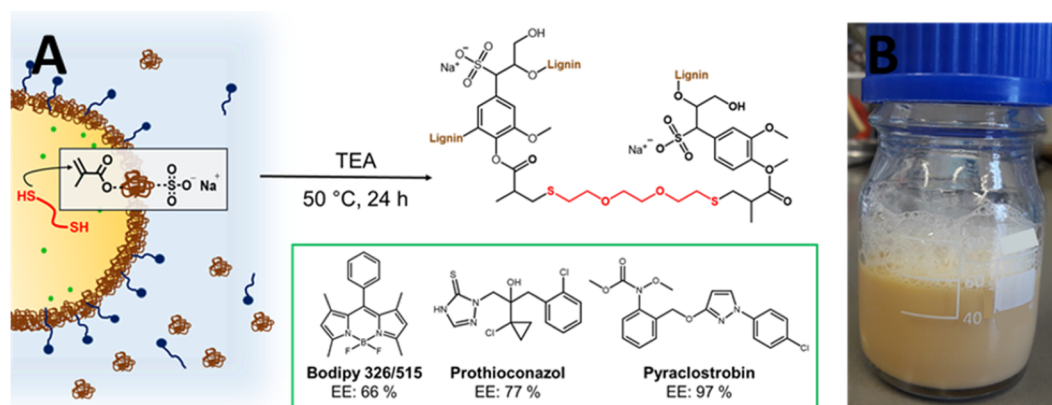


Figure 2. (A) Reaction scheme for the formation of lignin nanocarriers from methacrylated lignin sulfonate by interfacial cross-linking with a dithiol in miniemulsion. The encapsulated model drug Bodipy 326/515 and the fungicides prothioconazole and pyraclostrobin as well as the respective EE (EE measured by extraction) are shown. (B) Photograph of ca. 50 mL of dispersion containing cross-linked lignin sulfonate nanocarriers loaded with prothioconazole (solid content ca. 1 wt %).

to a general literature protocol.²⁷ Typically, more than 90% functionalization of the hydroxyl groups was achieved (i.e., 12–18 mmol/g methacrylates), which allows further chemical functionalization or cross-linking (Table 2). Only LSNa2 resulted in a degree of functionalization of 73%, that is, ca. 6 mmol methacrylate groups were attached per gram. Interestingly, for all samples, a higher conversion of phenolic than aliphatic hydroxyl groups was observed despite their lower nucleophilicity, which might be explained by steric reasons. For all modified lignin derivatives, the molar mass distribution in SEC shifted to lower elution times (i.e., higher molecular weights) relative to the pristine lignin sulfonate (Figure S4). FTIR spectroscopy further proved the successful modification of lignin sulfonates by the decreased $\nu(\text{OH}_{\text{arom.}})$ band at 3214 cm^{-1} and additional bands at 1736 and 1668 cm^{-1} , which correspond to the C=O and C=C stretching band of the methacrylic groups, respectively (Figure S5).

Nanocarrier Preparation. An efficient cross-linking at the droplet interface of a miniemulsion requires interfacially active monomers.²⁹ As all lignin sulfonates are interfacially active, they are suitable reactive surfactants. The interfacial tension between water and cyclohexane in the presence of modified lignin sulfonates was quantified by spinning drop tensiometry. At a concentration of 5 mg/mL, the methacrylated lignin sulfonates were able to decrease the interfacial tension from 44.0 mN/m to ca. 12–14 mN/m (cf. Table S1). Hence, the functionalized lignin sulfonates showed an interfacial activity that is comparable to the common nonionic surfactants, for example, Lutensol AT50 (12 mN/m at $c = 5$ mg/mL). The sample LSNa1-MA decreased the interfacial tension to 6.6 mN/m, which is similar to the value determined, for example, for the anionic surfactant sodium dodecyl sulfate (SDS, 5 mN/m at $c = 5$ mg/mL). For the nanocarrier preparation, LSNA1-MA was used. The comparison of molecular weight and functional groups of each methacrylated lignin sulfonate gave no clear explanation for the exceptional position of LSNA1-MA, though. It is noticeable, however, that the latter compound is only one without phenolate groups (Table S1).

Lignin nanocarriers were prepared by cross-linking methacrylated lignin sulfonate (LSNA1-MA) at the droplet interface of a direct miniemulsion (Figure 2): the water-insoluble dithiol cross-linker EDBET was dissolved with an additional hydrophobic cargo in cyclohexane or rapeseed oil (see below) as the

dispersed phase. Afterward, the mixture was added to an aqueous solution containing methacrylated lignin sulfonate, the alkaline catalyst TEA, and an additional surfactant (SDS or the nonionic Lutensol AT50). To generate a colloidal stable miniemulsion, the two-phase mixture was sonicated under ice cooling and a brownish miniemulsion was obtained. The polyaddition at the interface of the dispersed oil droplets was initiated by increasing the temperature to 50 °C. The reaction was allowed to proceed under vigorous stirring for ca. 15 h, yielding a colloidal stable dispersion, with a solid content of ca. 10 mg/mL. The product was stored in a closed vial (to prevent the evaporation of cyclohexane). The dispersions of the lignin sulfonate nanocarriers were stored for several weeks at room temperature (ca. 22 °C) in the dark and no aggregation was detected by dynamic light scattering; in fact, the measured diameters by DLS remained constant.

The formation of an insoluble polymer indicated the chemical cross-linking of the methacrylated lignin sulfonate during the reaction. FTIR spectroscopy after washing and lyophilization further proved the covalent cross-linking of the nanocarriers during the thio-Michael reaction. Figure 3 shows an overlay of the IR spectra of the native lignin sulfonate, the methacrylated lignin sulfonate, and the nanocarriers (after washing and lyophilization). The spectrum of the brownish solid (red curve in Figure 3) confirmed the reaction of the

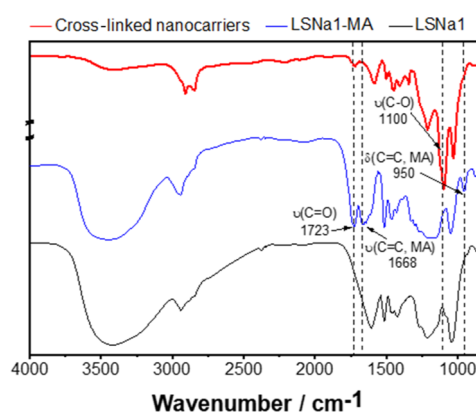


Figure 3. FTIR spectrum of nanocarriers prepared by interfacial cross-linking of methacrylated lignin sulfonate using cyclohexane as the dispersed phase (reaction condition no. 4, see Table 3).

Table 3. Reaction Conditions for the Formation of Lignin Nanocarriers from Methacrylated Lignin Sulfonate^a

no.	surfactant	c(TEA)/mmol/mL	c(CL)/mmol/mL	oil phase	cargo	diameter/nm (PDI)	EE %
1		0.066	0.060	cyclohexane	pyraclostrobin	467 (0.24)	95
2	SDS		0.060	cyclohexane		270 (0.22)	
3	Lutensol AT50		0.060	cyclohexane		240 (0.26)	
4	SDS	0.066	0.132	cyclohexane	Bodipy	250 (0.02)	66
5	SDS	0.054	0.108	cyclohexane	Bodipy	240 (0.09)	67
6	SDS	0.042	0.084	cyclohexane	Bodipy	240 (0.04)	66
7	SDS	0.030	0.060	cyclohexane	Bodipy	250 (0.07)	66
8	SDS	0.066	0.132	rapeseed oil		200 (0.23)	
9	SDS	0.066	0.132	rapeseed oil	pyraclostrobin	polymodal	97
10	SDS	0.066	0.132	rapeseed oil	prothioconazol	207 (0.32)	77

^aDiameters and PDI determined by DLS. The encapsulation efficiency (EE %) was measured after extraction from the dispersion with cyclohexane either photometrically for Bodipy or by HPLC for prothioconazole and pyraclostrobin; TEA = triethylamine, CL = cross-linker.

methacrylate moieties with the thiol groups of the EDBET cross-linker by a decreased intensity of the stretching (1668 cm^{-1}) and bending (950 cm^{-1}) band of the $\text{C}=\text{C}$ double bond relative to the signal of the carbonyl stretching motion at 1723 cm^{-1} . Additionally, we found an intense $\text{C}-\text{O}$ stretching signal of EDBET's glycol moiety at 1100 cm^{-1} , which further suggests the successful incorporation of the cross-linker (Figure 3).³⁰

Further, the effect of surfactant, cargo, base catalyst, oil phase, and amount of the cross-linking agent on nanocarrier formation was studied (Table 3). Typically, nanocarriers with diameters between 200 and 300 nm and a moderate size distribution were obtained [PDI < 0.32 (mostly below 0.1), Table 3]. TEM proved the formation of spherical nanoparticles with a core-shell morphology, indicating that the reaction between methacrylates and thiols was triggered mainly at the droplet interface (Figures 4A and S8). The reaction proceeded in the presence or without the addition of the basic catalyst TEA; however, we assume that reaction kinetics were increased in the presence of the catalyst. When we added a cargo to the miniemulsion, in all cases, lower polydispersity values were obtained as the cargo might act as an additional costabilizer (ultrahydrophobe). In general, the addition of a small amount of the costabilizer, which is a low molecular weight, highly water-insoluble component such as hexadecane, prevents Ostwald ripening, a process by which droplets disappear by monomer diffusion from small to large droplets.³¹ No significant difference regarding particles size distribution was observed by DLS when stabilizing the emulsion with SDS or with Lutensol AT50. The stabilization only with the amphiphilic methacrylated lignin and without an additional surfactant led to slightly larger particle sizes according to DLS, probably because of some aggregation or interparticle cross-linking but no sedimentation or macroscopic aggregation was observed even after several weeks of storage (Table 3, no. 1, Figure S6A).

Agrochemical Loading and Release. To apply the nanocarriers for drug delivery, the formulation must allow encapsulation and controlled release of the active ingredients. We first encapsulated the hydrophobic dye Bodipy 326/515 as a model drug and investigated the release kinetics. To adjust the speed of diffusion from the nanocarriers to the aqueous phase, we generated nanocarriers with varying cross-linking density by a stepwise reduction of EDBET from 1.1 to 0.5 equiv relative to the amount of methacrylate groups. The encapsulation of Bodipy 326/515 ($24\text{ }\mu\text{g/mL}$) did not change the average size distribution compared to "empty" lignin NCs

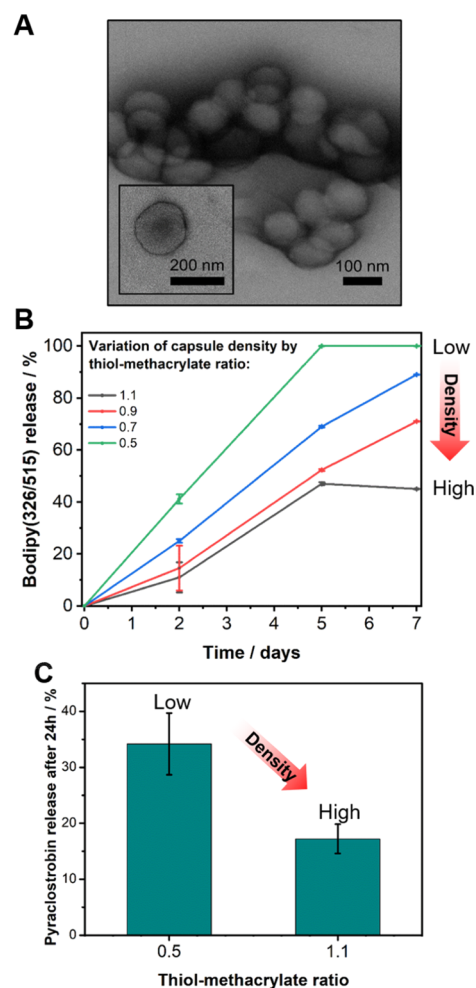


Figure 4. (A) TEM image of cross-linked nanocarriers (entry 4, Table 3) showing a core-shell morphology. (B) Release profile of Bodipy 326/515 from lignin sulfonate nanocarriers prepared with different amounts of cross-linkers (release by diffusion was determined by extraction of "free" dye with cyclohexane). (C) Release of pyraclostrobin after 24 h from lignin sulfonate nanocarriers prepared with different amounts of cross-linkers (release diffusion was determined by extraction of "free" fungicide with cyclohexane).

but decreased the PDI as the dye most likely acted as a ultrahydrophobe reducing Ostwald ripening (Table 3, no. 4–7). To determine the EE of the hydrophobic cargo, two different approaches were used: (A) nanocarriers were centrifuged and the supernatant was analyzed for Bodipy

326/515 (either dissolved or solubilized in micelles). (B) Cyclohexane was used to extract either the dye or the fungicide pyraclostrobin from the dispersion; this approach also detects surface-adsorbed or precipitated cargo. However, parts of the encapsulated cargo might also be extracted, so that the actual EE might be underestimated in this case. Using method A, an encapsulation of more than 90% was measured, independent from the amount of the cross-linker. As the used Bodipy has very low water solubility, the residual 10% is adsorbed most likely on the nanocarrier surface or dispersed in micelles in the continuous phase. As expected, a lower value of ca. 70% was determined for all nanocarriers when measuring the EE after extraction (method B). Noticeably, the amount of the cross-linker did not influence the amount encapsulated cargo but had effect on the release kinetics because of different diffusivities through the cross-linked membrane (Figure 4B). The release of the active ingredient was measured after 2, 5, and 7 days by washing the dispersion with cyclohexane and subsequent quantification of Bodipy 326/515 transferred to the cyclohexane phase (analog to method B). The cross-linking directly affected the release kinetics of the cargo: Using thiol and methacrylate groups in a ratio of 0.5, the encapsulated Bodipy 326/515 was released completely after 5 days. Increasing the ratio stepwise to 1.1 equiv, the release rate was reduced systematically to ca. 60% (0.7 equiv), 52% (0.9 equiv), or 45% (1.1 equiv), which suggests the formulation of nanocarriers with higher degree of cross-linking that resulted in lower diffusion from the nanocarriers. Cross-linking density also affected the release behavior for pyraclostrobin: nanocarriers with a high cross-linking density released significantly less of the fungicide after 24 h than nanocarriers with a lower cross-linking density (Figure 4C). Hence, the formulation provides a time-controlled release of the cargo via diffusion. To prevent premature release of the cargo, for example, during storage, the nanocarriers were centrifuged (4000 rpm, 30 min) and the aqueous supernatant was removed. The wet pellet allows storage without drug loss and can be redispersed easily in a 1 mg/mL SDS solution by vigorous shaking to yield a stable dispersion (ca. 10 mg in 1 mL solution). According to DLS, the centrifugation did not change the particle size distribution (Figure S7).

As the nanocarrier dispersion is composed on a plant-based, abundant, and cheap raw material, the approach might be of interest as a formulation for agrochemicals. We therefore replaced cyclohexane with rapeseed oil as a sustainable solvent for hydrophobic fungicides. The plant oil is nontoxic and does not need to be removed prior application. The oil contains unsaturated fatty acids offering additional points for cross-linking. However, because of the relatively low electrophilicity of the double bonds and lignin's radical scavenger properties,³² no reaction via Michael- or thiol-ene-addition is likely.³³

Using plant oil as a hydrophobic phase, colloidal stable dispersions were obtained, which did not phase-separate even after several weeks of storage. As the formed nanocarriers had an average diameter of 200 nm and a PDI of 0.23, rapeseed oil was considered as a sustainable alternative to cyclohexane (Table 3, no. 8). Likewise, the oil was found as a good solvent for the broad-spectrum fungicides prothioconazole (ca. 30 mg/mL at 25 °C) and pyraclostrobin (ca. 50 mg/mL at 25 °C). We also encapsulated two commercially available systemic fungicides (pyraclostrobin and prothioconazole) into the lignin sulfonate nanocarriers, which are currently used in spraying applications for wheat, almonds, peanuts, oats, and so forth.³⁴

When adding EDBET to the mixture, the solubility of prothioconazole further increased (to ca. 70 mg/mL at 25 °C), while the solubility of pyraclostrobin remained unchanged. At a loading of 0.5 mg/mL (regarding to the total volume of the dispersion), stable dispersions were obtained in both cases. Prothioconazole-loaded nanocarriers had an average diameter of 207 nm and a monomodal size distribution, whereas a polymodal size distribution was monitored for nanocarriers loaded with pyraclostrobin (Table 3, entries 9 and 10; Figure S6C). These differences might be explained by the lower solubility of pyraclostrobin in the dispersed phase or some aggregation. The EEs were determined by extraction of the free fungicide with cyclohexane (see method B above) and quantified their amounts by HPLC. For both fungicides, high EEs with 97% for pyraclostrobin and 77% for prothioconazole were detected, proving the herein developed nanoformulation as a promising tool for drug delivery in sustainable plant protection.

CONCLUSIONS

Lignin sulfonates were efficiently methacrylated and subsequently cross-linked by thia-Michael addition with a dithiol in a miniemulsion. Even if all lignin sulfonates exhibited different molar masses, numbers of hydroxyl groups, and molecular structures, typically more than 90% of the hydroxyl groups were methacrylated. The methacrylated and amphiphilic lignin sulfonates were readily soluble in water and were able to stabilize emulsions of cyclohexane or plant oils in water. Cross-linking at the interface of these droplets generated nanocarriers with a core-shell morphology, which were loaded with the fungicides pyraclostrobin or prothioconazole. As the nanocarriers are composed mainly of the bio-based and biodegradable resources lignin and oils, they might find application as sustainable nanoformulations for controlled delivery of agrochemicals without the risk of microplastic pollution, for example, for spraying applications or trunk injections.

ASSOCIATED CONTENT

Supporting Information

The Supporting Information is available free of charge at <https://pubs.acs.org/doi/10.1021/acssuschemeng.0c05897>.

Additional characterization data from NMR and FTIR spectra, TEM images, SEC, and HPLC elugrams (PDF)

AUTHOR INFORMATION

Corresponding Author

Frederik R. Wurm – Max-Planck-Institut für Polymerforschung, 55128 Mainz, Germany; Sustainable Polymer Chemistry Group, MESA+ Institute for Nanotechnology, Faculty of Science and Technology, Universiteit Twente, 7500 AE Enschede, The Netherlands; orcid.org/0000-0002-6955-8489; Phone: +31534895169; Email: frederik.wurm@utwente.nl

Authors

Sebastian Beckers – Max-Planck-Institut für Polymerforschung, 55128 Mainz, Germany
Stefan Peil – Max-Planck-Institut für Polymerforschung, 55128 Mainz, Germany

Complete contact information is available at: <https://pubs.acs.org/doi/10.1021/acssuschemeng.0c05897>

Notes

The authors declare no competing financial interest.

ACKNOWLEDGMENTS

This project is part of the BIOrescue project, which has received funding from the Bio-Based Industries Joint Undertaking under the European Union's Horizon 2020 research and innovation program under grant agreement no. 720708.

REFERENCES

- (1) Kumar, V.; Kumar, P. Pesticides in agriculture and environment: Impacts on human health. *Contaminants in Agriculture and Environment: Health Risks and Remediation*; Agro Environ Media, Publication Cell of AESA, Agriculture and Environmental Science Academy, 2019; Vol. 1, p 76.
- (2) Mulqueen, P. Recent advances in agrochemical formulation. *Adv. Colloid Interface Sci.* **2003**, *106*, 83–107.
- (3) Camara, M. C.; Campos, E. V. R.; Monteiro, R. A.; do Espírito Santo Pereira, A.; de Freitas Proença, P. L.; Fraceto, L. F. Development of stimuli-responsive nano-based pesticides: emerging opportunities for agriculture. *J. Nanobiotechnol.* **2019**, *17*, 100.
- (4) Bartolucci, C.; Antonacci, A.; Arduini, F.; Moscone, D.; Fraceto, L.; Campos, E.; Attaallah, R.; Amine, A.; Zanardi, C.; Cubillana-Aguilera, L. M.; Palacios Santander, J. M.; Scognamiglio, V. Green nanomaterials fostering agrifood sustainability. *TrAC, Trends Anal. Chem.* **2020**, *125*, 115840.
- (5) Rinaldi, R.; Jastrzebski, R.; Clough, M. T.; Ralph, J.; Kennema, M.; Bruijninx, P. C. A.; Weckhuysen, B. M. Wege zur Verwertung von Lignin: Fortschritte in der Biotechnik, der Bioraffination und der Katalyse. *Angew. Chem.* **2016**, *128*, 8296–8354.
- (6) Delidovich, I.; Hausoul, P. J. C.; Deng, L.; Pfitzenreuter, R.; Rose, M.; Palkovits, R. Alternative Monomers Based on Lignocellulose and Their Use for Polymer Production. *Chem. Rev.* **2016**, *116*, 1540–1599.
- (7) Tao, J.; Li, S.; Ye, F.; Zhou, Y.; Lei, L.; Zhao, G. Lignin – An underutilized, renewable and valuable material for food industry. *Crit. Rev. Food Sci. Nutr.* **2019**, *60*, 2011–2033.
- (8) Yiamsawas, D.; Beckers, S. J.; Lu, H.; Landfester, K.; Wurm, F. R. Morphology-Controlled Synthesis of Lignin Nanocarriers for Drug Delivery and Carbon Materials. *ACS Biomater. Sci. Eng.* **2017**, *3*, 2375–2383.
- (9) Beisl, S.; Miltner, A.; Friedl, A., Lignin from Micro- to Nanosize: Production Methods. *Int. J. Mol. Sci.* **2017**, *18* (), DOI: 10.3390/ijms18061244.
- (10) Iravani, S.; Varma, R. S. Greener synthesis of lignin nanoparticles and their applications. *Green Chem.* **2020**, *22*, 612–636.
- (11) Meier, D.; Zúñiga-Partida, V.; Ramírez-Cano, F.; Hahn, N.-C.; Faix, O. Conversion of technical lignins into slow-release nitrogenous fertilizers by ammoxidation in liquid phase. *Bioresour. Technol.* **1994**, *49*, 121–128.
- (12) Sadeghi, N.; Shayesteh, K.; Lotfiman, S. Effect of Modified Lignin Sulfonate on Controlled-Release Urea in Soil. *J. Polym. Environ.* **2017**, *25*, 792–799.
- (13) Pishnamazi, M.; Hafizi, H.; Shirazian, S.; Culebras, M.; Walker, G.; Collins, M. Design of Controlled Release System for Paracetamol Based on Modified Lignin. *Polymers* **2019**, *11*, 1059.
- (14) Dessbesell, L.; Paleologou, M.; Leitch, M.; Pulkki, R.; Xu, C. Global lignin supply overview and kraft lignin potential as an alternative for petroleum-based polymers. *Renew. Sustain. Energy Rev.* **2020**, *123*, 109768.
- (15) Tribot, A.; Amer, G.; Abdou Alio, M.; de Baynast, H.; Delattre, C.; Pons, A.; Mathias, J.-D.; Callois, J.-M.; Vial, C.; Michaud, P.; Dussap, C.-G. Wood-lignin: Supply, extraction processes and use as bio-based material. *Eur. Polym. J.* **2019**, *112*, 228–240.
- (16) Sipponen, M. H.; Lange, H.; Crestini, C.; Henn, A.; Österberg, M. Lignin for Nano- and Microscaled Carrier Systems: Applications, Trends, and Challenges. *ChemSusChem* **2019**, *12*, 2039–2054.
- (17) Beisl, S.; Miltner, A.; Friedl, A. Lignin from Micro- to Nanosize: Production Methods. *Int. J. Mol. Sci.* **2017**, *18*, 1244.
- (18) Machado, T. O.; Beckers, S. J.; Fischer, J.; Müller, B.; Sayer, C.; de Araújo, P. H. H.; Landfester, K.; Wurm, F. R. Bio-Based Lignin Nanocarriers Loaded with Fungicides as a Versatile Platform for Drug Delivery in Plants. *Biomacromolecules* **2020**, *21*, 2755–2763.
- (19) Antonietti, M.; Landfester, K. Polyreactions in miniemulsions. *Prog. Polym. Sci.* **2002**, *27*, 689–757.
- (20) Yiamsawas, D.; Baier, G.; Thines, E.; Landfester, K.; Wurm, F. R. Biodegradable lignin nanocontainers. *RSC Adv.* **2014**, *4*, 11661.
- (21) Beckers, S. J.; Dallo, I. A.; del Campo, I.; Rosenauer, C.; Klein, K.; Wurm, F. R. From Compost to Colloids—Valorization of Spent Mushroom Substrate. *ACS Sustainable Chem. Eng.* **2019**, *7*, 6991–6998.
- (22) Chen, N.; Dempere, L. A.; Tong, Z. Synthesis of pH-Responsive Lignin-Based Nanocapsules for Controlled Release of Hydrophobic Molecules. *ACS Sustainable Chem. Eng.* **2016**, *4*, 5204–5211.
- (23) Fischer, J.; Beckers, S. J.; Yiamsawas, D.; Thines, E.; Landfester, K.; Wurm, F. R. Targeted Drug Delivery in Plants: Enzyme-Responsive Lignin Nanocarriers for the Curative Treatment of the Worldwide Grapevine Trunk Disease Esca. *Adv. Sci.* **2019**, *6*, 1802315.
- (24) Demuner, I. F.; Colodette, J. L.; Demuner, A. J.; Jardim, C. M. Biorefinery review: Wide-reaching products through kraft lignin. *BioResources* **2019**, *14*, 7543–7581.
- (25) Naseem, A.; Tabasum, S.; Zia, K. M.; Zuber, M.; Ali, M.; Noreen, A. Lignin-derivatives based polymers, blends and composites: A review. *Int. J. Biol. Macromol.* **2016**, *93*, 296–313.
- (26) L'udmila, H.; Andrea, Š.; Ház, A. Lignin, potential products and their market value. *Wood Res.* **2015**, *60*, 973–986.
- (27) Balakshin, M.; Capanema, E. On the Quantification of Lignin Hydroxyl Groups With³¹P and¹³C NMR Spectroscopy. *J. Wood Chem. Technol.* **2015**, *35*, 220–237.
- (28) Calvo-Flores, F. G.; Dobado, J. A. Lignin as renewable raw material. *ChemSusChem* **2010**, *3*, 1227–1235.
- (29) Piradashvili, K.; Alexandrino, E. M.; Wurm, F. R.; Landfester, K. Reactions and Polymerizations at the Liquid-Liquid Interface. *Chem. Rev.* **2016**, *116*, 2141–2169.
- (30) Wadhwa, P.; Kharbanda, A.; Sharma, A. Thia-Michael Addition: An Emerging Strategy in Organic Synthesis. *Asian J. Org. Chem.* **2018**, *7*, 634–661.
- (31) Asua, J. M. Miniemulsion polymerization. *Prog. Polym. Sci.* **2002**, *27*, 1283–1346.
- (32) Lu, F. J.; Chu, L. H.; Gau, R. J. Free radical-scavenging properties of lignin. *Nutr. Canc.* **1998**, *30*, 31–38.
- (33) Desroches, M.; Caillol, S.; Lapinte, V.; Auvergne, R.; Boutevin, B. Synthesis of biobased polyols by thiol–ene coupling from vegetable oils. *Macromolecules* **2011**, *44*, 2489–2500.
- (34) Anco, D. J.; Hiers, J. B.; Thomas, J. S. Improved Management Efficacy of Late Leaf Spot on Peanut Through Combined Application of Prothioconazole with Fluxapyroxad and Pyraclostrobin. *Agronomy* **2020**, *10*, 298.